A New Family of Microstrip Open-Loop Resonator Filters for High Selectivity Applications

†David Cañete Rebenaque, †Alejandro Alvarez Melcon and ‡Marco Guglielmi

†Technical University of Cartagena
Campus Muralla del Mar s/n
30202 Cartagena, Murcia, Spain.
E-mail: david.canete@upct.es
‡European Spacen Agency, ESA/ESTEC,
P.O. Box 299, Noordwijk, The Netherlands.

Key Words: Microwave filters, Microstrip filters, Microstrip resonators, Elliptic filters, Poles and zeros

Abstract

In this paper the design of a novel planar narrowband microstrip filter is presented. The structure is designed and manufactured in microstrip technology, and it is formed by set of pairs of resonators of different lengths. The length of one resonator in each pair is adjusted so that a suitable odd resonance is tuned to the center frequency of the filter. The length of the other resonator is adjusted so that the next even resonance is tuned again to the center frequency of the filter. The different path of the signal in each resonator produces a cancellation of energy at a given frequency, therefore implementing a transmission zero in the insertion loss response of the filter. First, this paper presents a design example of a single set of resonators (basic unit cell) working at the fifth and sixth resonances. Then, two basic unit cells working at the first and second resonances are first optimized, and then they are cascaded to show how higher order filter responses can be implemented. Measured results confirm the theoretical predictions, and validate the new structures for high selectivity applications.

1 Introduction

Modern communications systems often call for frequency selective components with sharp cutoff slopes to separate adjacent channels and prevent cross-talk [1]. In the design of filters, of paramount relevance is the filter selectivity, which must be increased in order to better reject spurious signals [2]. The selectivity can be increased by using filters whose response includes attenuation poles (transmission zeros) at finite frequencies in the insertion loss response [3, 4].

In printed technology, several previous works have been developed in order to increase the filter selectivity. For instance, in [5] a printed filter composed of square open-loop resonators is presented. In the structure, the transmission zeros are obtained by classical cross-coupling interactions between

nonadjacent resonators. The work proposed in [5] is based on previous works [6, 3], in which elliptic transfer functions are also implemented by using similar square open-loop resonators combined with cross couplings between nonadjacent resonators. Another example of a printed filter which uses side cross-coupling interactions can be found in [7], where hair pin resonators are placed in a square matrix to achieve an elliptic transfer function for a second-order filter.

In addition to the classical side-coupled implementation of transmission zeros, other approaches based on broadside couplings have been implemented. A very useful example can be found in [8], where an elliptic transfer function is synthesized for a second order filter by broadside coupling two resonators through a slot open on the common ground plane of a two layers microstrip structure. Also in [9] a three pole filter is presented with a transmission zero due to a broadside cross coupling between the first and third resonator. A different technique is used in [10], which uses $\lambda/4$ stubs for generating elliptic responses. Also in [11] transmission zeros are implemented with stub-tapped half-wavelength resonators.

In this paper we present an alternative procedure for the implementation of transmission zeros in the insertion loss response of microstrip printed filters. The main difference with respect to previous designs is that the transmission zero is obtained by providing more than one path to the signal between the input and output lines, so that destructive interference can take place. The structure is composed of sets of two open-loop resonators of different lengths. The first length is adjusted to tune a suitable odd resonance of the resonator to the center frequency of the filter. On the contrary, the second length is adjusted to tune the next even resonance of the resonator to the center frequency. The opposite phases occurring in the signal path from the input and output in both resonators produce a cancellation of energy at a given frequency, therefore creating the desired transmission zero.

The advantage of the proposed configuration with respect existing ones, is that several structures of the type just described can be easily cascaded to produce higher order responses. The in-line configuration created with this approach, leads to a structure in which the different sections have little or no influence on the others. As a consequence, each section can be optimized separately, and then connected to the final structure with little tuning or re-adjustment of the individual units. This advantage has already been recognized in [12], in the context of the study of the sensitivity of different configurations of coupled resonator filters.

The structure proposed in this paper is based on the same design strategy as presented in [13]. In [13], however, the technique is applied to the design of dual mode filters in waveguide technology. The extension of this technique to planar printed microstrip structures shows to lead to very compact and useful microwave filters exhibiting high selectivity. This idea was also proposed in [14] in the context of novel coupling schemes to achieve elliptic transfer functions, but no implementations were reported.

In this paper the design strategy of a simple two order filter is presented, together with the procedure to cascade and optimize several basic configurations in order to obtain higher order structures with the desired responses. First, the two order filter prototype is manufactured, and results are discussed. Next, two different configurations of cascading two of these structures are proposed. One leads to a symmetrical geometry and places two transmission zeros on one side of the passband. The other alternative places one transmission zero at each side of the passband, and leads to a non-symmetrical geometry. This last configuration is very useful in applications when high rejection is required on

both sides of the passband. Measured results show that the structures presented are indeed feasible, exhibiting high selectivity and high rejection capabilities.

2 Structure Description

The basic configuration (basic unit cell) of the filter structure can be seen in Fig. 1. It consists on the input and output lines which are coupled in a shunted configuration to two open loop resonators of different lengths. One resonator is designed to work at a suitable odd resonance, while the other is designed to operate at the next even resonance. The interaction of the signal in both paths produces the required cancellation of energy at a given frequency, therefore leading to a transmission zero in the insertion loss response of the filter.

The two main geometrical parameters in this structure are the lengths of the resonators, whose approximated values are $N\,\lambda_{eff}/2$ and $(N+1)\,\lambda_{eff}/2$ respectively at the center frequency of the passband, where N is the selected operational resonance for the loops. By adjusting properly these two lengths, the cancellation of energy, and therefore the transmission zero, occurs in the proximity of the center frequency, leading to a sharp transition between the transmission and the cut-off bands.

In this structure the lengths L_{i_2} and L_{o_2} of Fig. 1, together with the gaps S_u, S_l, control the input and output couplings of the filter, and must be carefully adjusted to achieve the required bandwidth and desired in-band characteristics. Since the input and output lines are side coupled to the resonators, relatively narrow bandpass filters can be obtained. A final fine adjustment of this coupling is required to achieve the required level of insertion losses within the passband of the filter.

There are two main issues than need to be considered when selecting the value of N (order of the resonance in which the resonators operate). The first one is the insertion losses of the structure, together with the size of the resonators. Higher values of N lead to electrically bigger resonators. This can give better geometrical control for millimeter wave filters, where dimensions are very small. On the contrary, the insertion loss response of the filter deteriorates as N increases. We have experienced a 1.4dB increment in the insertion losses of the structure, each time the order of the resonance N is increased by one. The second important issue is for the special case when $N = 1$. In this case the length of the whole loop resonator is only $\lambda_{eff}/2$. This means that the input/output coupling lengths, L_{i_2} and L_{o_2} of Fig. 1 need to be considerably smaller than $\lambda_{eff}/2$. This results in rather small input/output coupling values that can be achieved with this configuration. If the amount of input/output couplings that can be achieved is not enough for your application, then a design with $N = 2$ is required. From this point you can select higher N values if you need to gain control over the physical dimensions of the resonators, but at the expense of additional insertion losses.

Finally, by cascading several basic unit cells shown in Fig. 1 higher order filter responses can be easily optimized. Due to the in-line configuration, the different sections of the filter have very small influence on the other sections. This allows to optimize each section separately, with subsequent interconnection of the different sections, reducing or minimizing the final tuning of the whole structure. In the next section the design procedure for the basic unit cell shown in Fig. 1 will be first described, and then we will show how the basic unit cells can be cascaded in two different configurations to produce transmission zeros in one or both sides of the filter passband. Each alternative can be most

conveniently used in applications where high rejection is needed either in one side or in both sides of the passband.

3 Design Procedure

For the design of the basic unit cell shown in Fig. 1, first the input and output lines width is chosen so as to synthesize 50Ω microstrip lines. Then the lengths of the resonators are calculated to tune the required odd and next-even resonances respectively at the center frequency of the filter. For the design of the loop resonators, the length of the coupled lines (L_{i_2} and L_{o_2}), as well as the width of the gaps (S_u, S_l), must be carefully selected to achieve the required signal coupling (bandwidth of the filter). In the examples shown in this paper we have selected a gap width of $S_u = S_l = 0.2$mm so that the manufacturing process does not become critical. Also the separation between input and output lines must be high enough to avoid direct coupling between the input and output ports. A direct coupling between the input and output lines could degrade the overall filter performance.

If above considerations are taken into account, the optimization of the basic unit cell shown in Fig. 1 involves only a final adjustment of the length of the resonators L_{r_1} and L_{r_2}. The difference between the two lengths will control the position of the transmission zero, as well as the level of the reflection coefficient of the filter inside its passband (ripple). This is an interesting feature of the configuration proposed, since the position of the transmission zero can be easily shifted from one side of the passband to the other side, by just modifying the ratio between the lengths of the two resonators. Fig. 2 shows a basic unit cell in Fig. 1 optimized to produce a transmission zero above the passband. For this design the two resonators operate at $N = 1$ and $N = 2$ resonances respectively. If the length of the longer resonator is slightly increased with respect the shorter resonator, then the response is shown in Fig. 3, where the transmission zero is located now below the passband.

In the filter configuration proposed, we have a trade off between the value of the constant ripple inside the passband and the position of the transmission zero out of the passband. If the lengths of the resonators are adjusted so as to decrease the coupling between the two poles, then a lower reflection coefficient is obtained, but at the expense of a lower bandwidth since the transmission zero approaches to the passband. On the other hand, by increasing the coupling between the reflection poles, a wider matching bandwidth can be obtained with higher level of reflection coefficient, but the rejection capabilities of the filter are worse since the transmission zero moves apart from the passband.

In addition, independent control of the passband characteristics and the position of the transmission zero can be achieved by acting on the input and output coupling. If input/output coupling is increased, for instance by decreasing S_u and S_l, then the bandwidth of the filter will increase. Moreover, independent control on the level of return loss (S_{11}) can be achieved by adjusting asymmetrically the gaps S_l and S_u. To illustrate this last property, we present in Fig. 4 the response of the filter in Fig. 2 for three different values of the S_u and S_l gaps. It can be seen that the position of the transmission zero is essentially the same in all cases. Also the level of return losses within the passband is the same (-20dB), but the relative bandwidth of the filter has varied from 0.85% ($S_u = 0.29$mm, $S_l = 0.30$mm) to 2.5% ($S_u = 0.11$mm, $S_l = 0.10$mm).

Once the single filter has been designed, two identical unit cells can be cascaded to obtain a higher-

order response in a compact structure. Both high selectivity and bandwidth can simultaneously be obtained by cascading two of these novel filters configurations as shown in Fig. 5. The two basic structures whose responses are shown in Fig. 2 and Fig. 3 will be used as starting points for the design of more complex four pole bandpass filters. If two unit cells of the type shown in Fig. 2 are cascaded, then a four order filter is obtained. It should be noted that the geometry is completely symmetric from input to output, and that the transmission zeros due to both basic unit cells lie on the same side of the passband. An alternative design can be foreseen, if a unit cell of the type in Fig. 2 is cascaded with a unit cell of the type in Fig. 3. This last structure can be used when high rejection is to be obtained on both sides of the passband, since then a complete elliptic transfer function is obtained with one transmission zero at each side of the passband. On the contrary the complexity of the design increases, since this last concept leads to a non-symmetric structure.

Once the basic unit cells are optimized, the cascading process only involves the optimization of two extra parameters. The first one is the distance L_d between the two set of resonators (see Fig. 5). For the symmetric configuration, this length can be adjusted to control the balance between the two pair of resonances produced by each basic unit cell. The other important parameter is the width of the coupling line joining the two unit cells (W_d in Fig. 5). For the symmetric configuration this width can be decreased in order to adjust properly the inter-resonator coupling between the two set of resonances. By adjusting this width, a final equal-ripple filter response can be achieved throughout the whole passband. This last step simplifies considerably the optimization of higher order filter responses since only two extra parameters need to be optimized at each step.

For the non-symmetric configuration the final optimization also involves the adjustment of the same geometrical parameters. However, due to the non-symmetric nature of the structure, the effects of both L_d and W_d are coupled to each other. To show this behavior we present in Fig. 6 and Fig. 7 the response of the filter when L_d and W_d are varied respectively. As can be seen in Fig. 6, the variation of L_d affects not only to the balance of the two pair of resonances, but also to the coupling between them. In addition L_d also affects the attenuation slope that can be achieved out of the bandpass. It is observed in Fig. 6 that a sharper attenuation slope out of the passband (better rejection) is achieved with increasing L_d length. On the contrary, improvements in the reflection coefficient are obtained by reducing L_d. The final adjustment of this length, therefore, must be carried out on the basis of this trade off. Furthermore, in Fig. 7 we also observe that W_d affects not only to the inter-resonator coupling between the two pair of resonances, but also to the balance between them. Finally, it is observed in Fig. 7 that also this parameter affects the balance between the two attenuation slopes above and below the passband due to the transmission zeros. By adjusting properly W_d we can place both transmission zeros symmetrically, therefore obtaining the same degree of rejection above and below the passband of the filter.

The thick solid line in Fig. 6 and Fig. 7 corresponds to the final optimized structure. It can be seen that by adjusting L_d and W_d a constant ripple characteristic has been obtained inside the passband, together with symmetric transmission zeros on both sides of the passband, and with rejection levels of -27dB out of the passband due to the effect of the two transmission zeros. In spite of being a complex non-symmetric structure, the adjustment of these two parameters leads to constant-ripple elliptic filter response with high selectivity and transmission zeros symmetrically disposed on both sides of the passband.

4 Results

The full wave electromagnetic analysis tool employed for the simulation and optimization of the filters was the HP-ADS software. The first prototype manufactured was a single stage filter, with two loop resonators operating with $N = 5$ and $N = 6$ higher order resonances respectively. The structure has been optimized following the basic simple steps shown in this paper. The structure has been manufactured on a TMM-4 substrate ($\epsilon_r = 4.5$ and thickness $h = 0.51$mm), with the layout and physical dimensions shown in Fig. 8.

Measured and simulated results are compared for the transmission and reflection responses of this filter. The simulated results were computed with the HP-ADS software tool simulation (which uses the infinite size multilayered media Green's functions [15]), while the measured results were obtained with an HP-8720-ES vector network analyzer. In Fig. 9 the results are compared for the scattering parameters of the filter. It can be seen good agreement except for a frequency shift of about 50 MHz. Also, since higher order resonances ($N = 5, 6$) have been used to optimize the passband of the filter, lower order resonances can be seen before the actual passband. Results show that the nearest lower order resonance occurs around 3.9 GHz. The optimization of a filter prototype with $N = 1$ will decrease further the total dimensions of the filter as compared to Fig. 8.

Measured results show that the filter has a bandwidth of 1.38% and center frequency f_0 of 4.43GHz. The passband ripple remains lower than 0.25dB. As expected, the two resonators produce a 2-pole response filter with sharp transition due to a transmission zero.

Once the single filter configuration has been designed, manufactured and successfully tested, the next step is to cascade two unit cells to obtain a higher order response in a compact structure. The two basic structures whose responses are shown in Fig. 2 and Fig. 3 are used as starting points for the design of more complex four pole bandpass filters. The structures were also optimized following the basic guidelines given above, which essentially involves the optimization of the length and width of the extra line connecting the two basic unit cells (L_d and W_d of Fig. 5). In this case we have used for the design two basic unit cells operating and the first and second resonances ($N = 1$) of the structure. Also we have now used a different substrate for the manufacturing of the filters, namely a Duroid RO-4003 substrate ($\epsilon_r = 4.5$ and the thickness $h = 0.51$mm).

A first filter was designed by cascading two identical unit cells of the type shown in Fig. 2, to produce two transmission zeros above the passband. Furthermore, a second filter was designed using one unit cell of the type shown in Fig. 2 and one of the type shown in Fig. 3, to produce one transmission zero at each side of the passband. The common dimensions of both filters are shown in Fig. 5. For the first design, both loop resonator are the same, and the branch dimensions shown in Fig. 5 take the following values: $L_{r_1} = L_{r_3} = 3.35$mm, and $L_{r_2} = L_{r_4} = 34.70$mm, with $W_d = 2.4$mm.

The second filter leads to a non-symmetric structure, and the dimensions in the second unit cell change to $L_{r_3} = 3.15$mm and $L_{r_4} = 35.45$mm, again with $W_d = 2.4$mm. As seen, the relation between the lengths of the resonators has increased for this second unit cell, and this produces the transmission zero below the passband. Finally, the distance between the two unit cells (L_d) is set to 10.6mm in the first case, and to 6.3mm for the second filter. The general aspect of the manufactured hardware obtained by cascading two unit cells can be seen in Fig. 12.

The results obtained are shown in Fig. 10 for the first design and in Fig. 11 for the second design. The figures show measured results and compare them with theorical predictions obtained with HP-ADS software. In the figures the theoretical predictions include losses in both the dielectric and in the metallic areas of the structure (finite conductivity). Measured results agree reasonably well with predictions. The measured responses exhibit higher bandwidth than expected. The differences are thought to be due to the assumption of infinite dielectric material by the software, and the imperfections of the PCB process (which was done with an LPKF *ProtoMat-C30S* milling machine).

5 Conclusions

In this paper we have presented a new microstrip filter structure exhibiting high selectivity. Unlike traditional designs, transmission zeros are implemented by providing more than one path to the signal between the input and output lines, so that destructive interference can take place. The basic structure consists of a two open-loop resonators of different lengths. The opposite phases of the signal in each resonator produces the cancellation of energy required for the implementation of a transmission zero. Single configurations as well as more complex filter prototypes, working at different resonances and manufactured on different substrates, have been designed, manufactured and tested. Two different four order filters have been proposed for maximum selectivity on one side or on both sides of the passband. Measured results confirm the validity and usefulness of the proposed configurations.

6 Acknowledgments

This work has been developed thanks to support of Spanish National projects ESP2001-4546-PE, TIC2000-0591-C03-03, and Regional Seneca project 2003.

References

[1] C.-Y. Chang and W.-C. Hsu, "Novel planar, square-shaped, dielectric-waveguide, single, and dual-mode filters," *IEEE Transactions on Microwave Theory and Techniques*, vol. 50, pp. 2527–2536, November 2002.

[2] J. S. Hong, M. J. Lancaster, D. Jedamzik, R. B. Greed, and J. C. Mage, "On the performance of HTS microstrip quasi-elliptic function filters for mobile communication application," *IEEE Transactions on Microwave Theory and Techniques*, vol. 48, pp. 1240–1246, 2000.

[3] C. C. Yu and K. Chang, "Novel compact elliptic-function narrow-band bandpass filters using microstrip open-loop resonators with coupled and crossing lines," *IEEE Transactions on Microwave Theory and Techniques*, vol. 46, pp. 952–958, 1998.

[4] D. Chambers and J. D. Rhodes, "Asymmtric synthesis of microwave filters," in *Proc. 11th European Microwave Conference*, (The Netherlands), pp. pp. 105–110, EuMC, September 7-11 1981.

[5] J. S. Hong and M. J. Lancaster, "Design of highly selective microstrip bandpass filters with a single pair of attenuation poles at finite frequencies," *IEEE Transactions on Microwave Theory and Techniques*, vol. 48, pp. 1098–1107, 2000.

[6] J. S. Hong and M. J. Lancaster, "Couplings of microstrip square open-loop resonators for cross-coupled planar microwave filters," *IEEE Transactions on Microwave Theory and Techniques*, vol. 44, pp. 2099–2109, 1996.

[7] J. S. Hong and M. J. Lancaster, "Cross-coupled microstrip hairpin-resonator filters," *IEEE Transactions on Microwave Theory and Techniques*, vol. 46, pp. 118–122, 1998.

[8] S. J. Yao, R. R. Bonetti, and A. E. Williams, "Generalized dual plane multicoupled line filters," *IEEE Transactions on Microwave Theory and Techniques*, vol. 41, pp. 2182–2189, 1993.

[9] A. A. Melcon, J. R. Mosig, and M. Guglielmi, "Efficient CAD of boxed microwave circuits based on arbitrary rectangular elements," *IEEE Transactions on Microwave Theory and Techniques*, vol. 47, pp. 1045–1058, July 1999.

[10] Y. A. S. Amari, K. Hamed and A. Freundorfer, "New elliptic microstrip $\lambda/4$ resonator filters," in *Proceedings of AMPC2001*, 2001.

[11] L. Zhu and W. Menzel, "Compact microstrip bandpass filter with two transmission zeros using a stub-tapped half-wavelength resonator," *IEEE Microwave and Wireless Components Letters*, vol. 13, pp. 16–20, January 2003.

[12] S. Amari and U. Rosenberg, "On the sensitivity of coupled resonator filters without some direct couplings," *IEEE Transactions on Microwave Theory and Techniques*, vol. 51, pp. 1767–1773, June 2003.

[13] M. Guglielmi, P. Jarry, E. Kerherve, O. Roquebrun, and D. Schmitt, "A new family of all-inductive dual-mode filters," *IEEE Transactions on Microwave Theory and Techniques*, vol. 49, pp. 1764–1769, October 2001.

[14] U. Rosenberg and S. Amari, "Novel coupling schemes for microwave resonators filters," *IEEE Transactions on Microwave Theory and Techniques*, vol. 50, pp. 2896–2902, December 2002.

[15] K. A. Michalski and J. R. Mosig, "Multilayered media green's functions in integral equation formulations," *IEEE Transactions on Antennas and Propagation*, vol. 45, pp. 508–519, 1997.

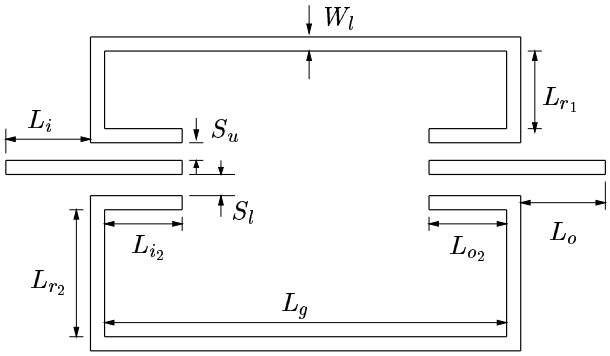

Figure 1: Filter layout of basic unit cell which produces one single transmission zero.

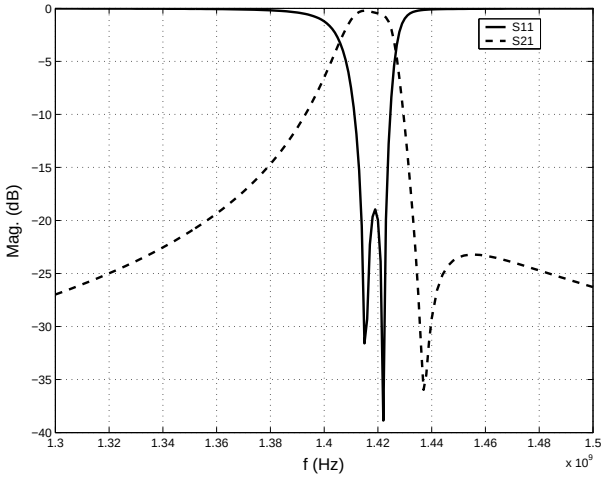

Figure 2: Basic response with one transmission zero above the passband. The dimensions are $L_i = L_o = 8.0$mm, $L_{i_2} = L_{o_2} = 10.4$mm, $L_g = 29.0$mm, $W_l = 2.5$mm, $L_{r_2} = 34.70$mm, $L_{r_1} = 3.35$mm, and $S_u = S_l = 0.2$mm. The relative dielectric constant is $\epsilon_r = 3.38$ and the thickness $h = 1.1$mm.

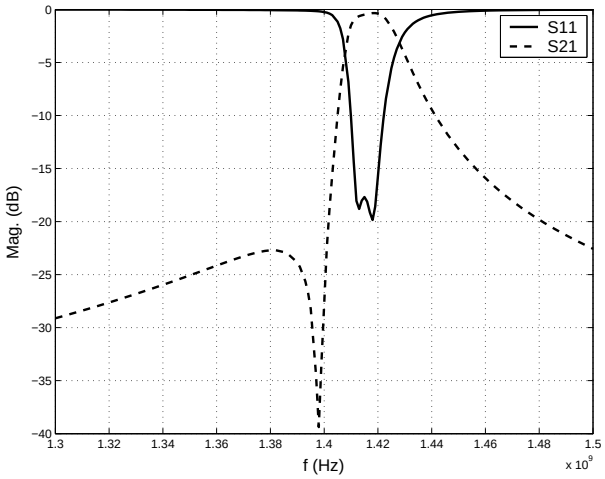

Figure 3: Basic response with one transmission zero below the passband. The dimensions are $L_i = L_o = 8.0$mm, $L_{i2} = L_{o2} = 10.4$mm, $L_g = 29.0$mm, $W_l = 2.5$mm, $L_{r_2} = 35.45$mm, $L_{r_1} = 3.15$mm, and $S_u = S_l = 0.2$mm. The relative dielectric constant is $\epsilon_r = 3.38$ and the thickness $h = 1.1$mm.

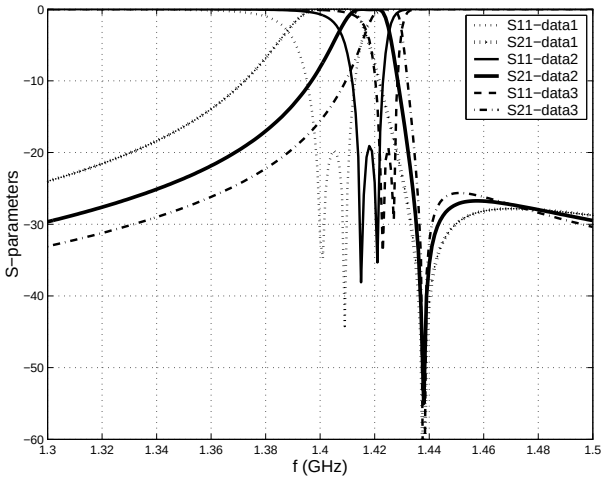

Figure 4: Filter response in Fig. 2 when input/output couplings are adjusted asymmetrically, showing independent control of bandwith, return loss level, and position of transmission zero. Data1: $S_u = 0.11$mm, $S_l = 0.10$mm; Data2: $S_u = 0.2$mm, $S_l = 0.2$mm; Data3: $S_u = 0.29$mm, $S_l = 0.30$mm.

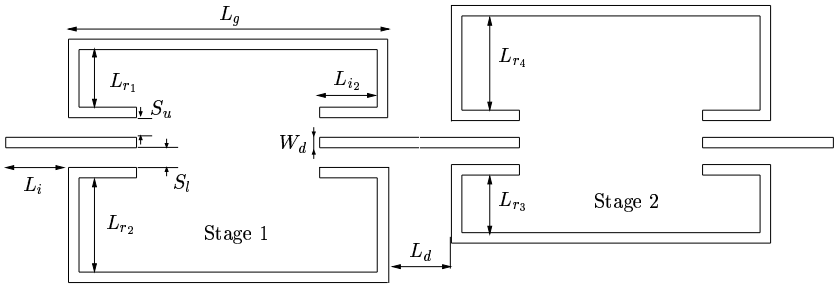

Figure 5: Filter with two cascaded basic unit cells. The common dimensions for the designs in this paper are: $L_i = 8$mm, $S_u = S_l = 0.2$mm, $L_{i_2} = 10.4$mm, $L_g = 34$mm. The relative dielectric constant is $\epsilon_r = 3.38$ and the thickness $h = 1.1$mm.

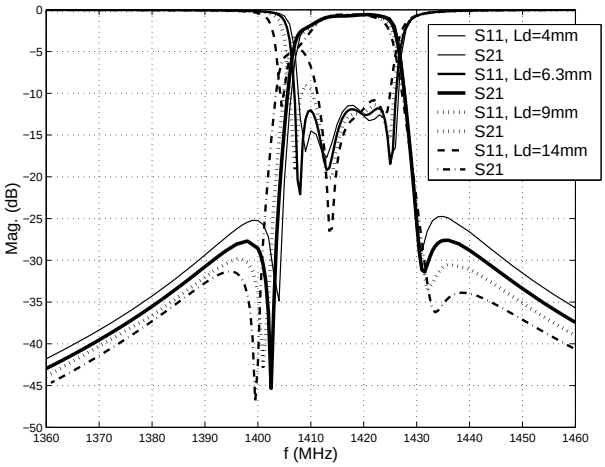

Figure 6: Effect of the variation of the distance between the two sets of resonators L_d.

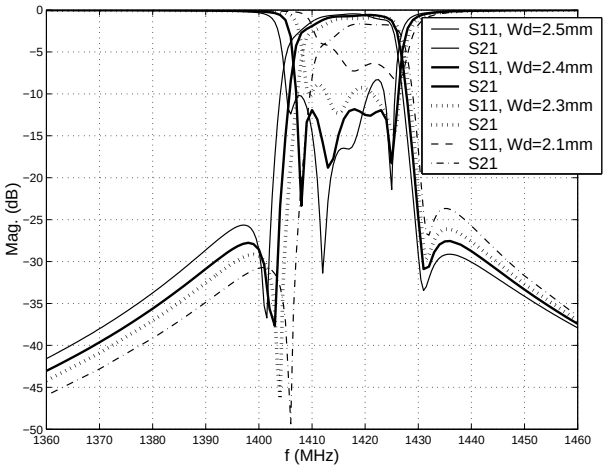

Figure 7: Effect of the variation of the line coupling width W_d.

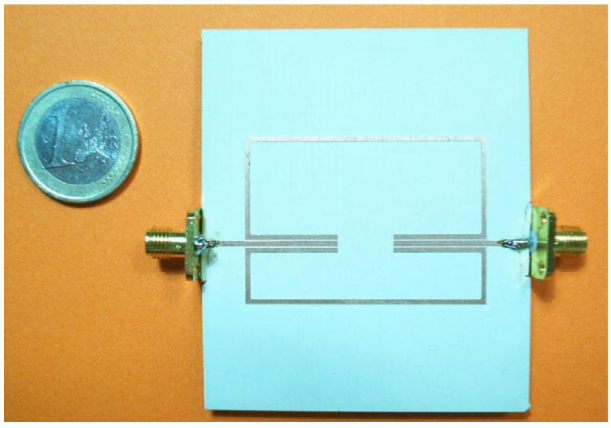

Figure 8: Manufactured filter prototype. The dimensions in Fig. 1 are $L_i = 8.0$mm, $L_o = 8.0$mm, $L_{i_2} = 16.0$mm, $L_{o_2} = 16.0$mm, $L_g = 42.0$mm, $W_l = 1.0$mm, $L_{r_2} = 16.8$mm, $L_{r_1} = 8.4$mm, and $S_u = S_l = 0.2$mm. The relative dielectric constant is $\epsilon_r = 4.5$ and the thickness $h = 0.51$mm.

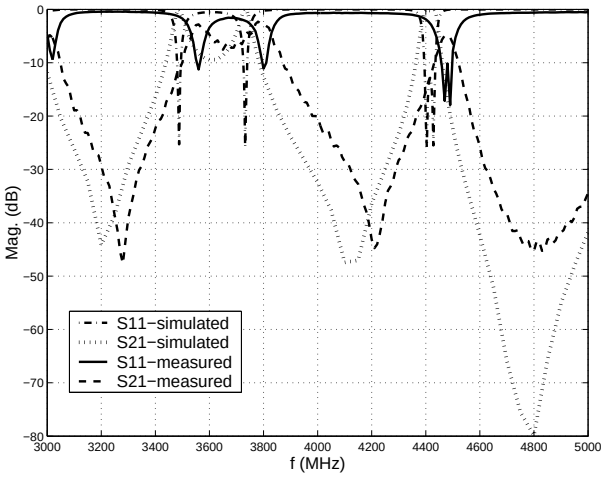

Figure 9: Measured and simulated S-parameters for the single-stage filter with $N = 5$.

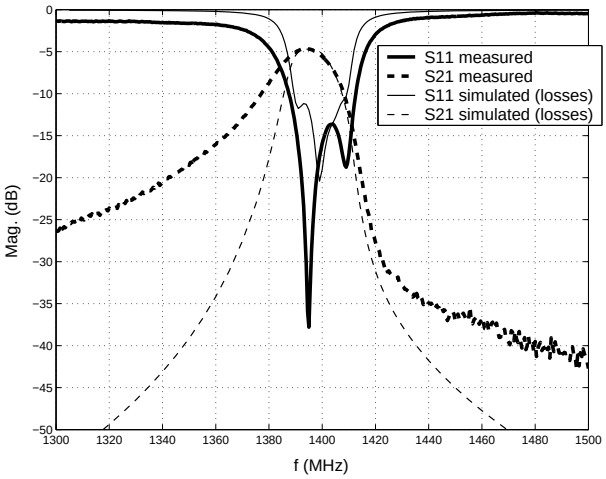

Figure 10: Measured and simulated results for a four pole filter with two transmission zeros above the passband. Results with losses are obtained with $\sigma = 10^{11} S/m$ and $\tan\delta = 0.0027$.

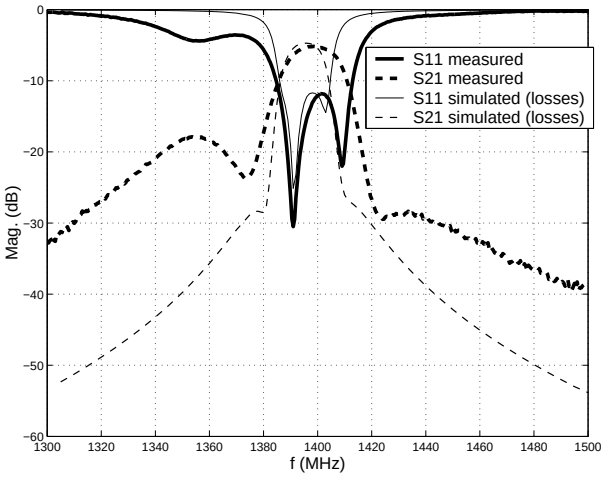

Figure 11: Measured and simulated results for a four pole elliptic filter with transmission zeros on both sides of the passband. Results with losses are obtained with $\sigma = 10^{11} S/m$ and $\tan\delta = 0.0027$.

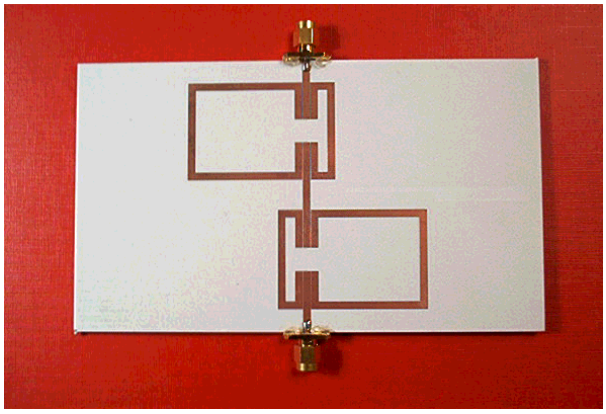

Figure 12: Image of the manufactured hardware obtained by cascading two basic unit cells of order two.